

Inflation of An Artery Leading to Aneurysm Formation and Rupture

J. S. Ren*

Abstract: Formation and rupture of aneurysms due to the inflation of an artery with collagen fibers distributed in two preferred directions, subjected to internal pressure and axial stretch are examined within the framework of nonlinear elasticity. A two layer tube model with a fiber-reinforced composite based incompressible anisotropic hyperelastic constitutive material is employed to model the stress-strain behavior of the artery wall with distributed collagen fibers. The artery wall takes up a uniform inflation deformation, and there are no aneurysms in the artery under the normal condition. But an aneurysm may be formed in arteries when the stiffness of the fibers is decreased to a certain value or the direction of the fibers is changed to a certain degree towards the circumferential direction. The aneurysm may expand to much large extent and become complex in shape. One portion of the aneurysm becomes highly distended as a bubble while the rest remains lightly inflated. The rupture of the aneurysm is discussed along with the distribution of stresses. Critical pressures and the rupture pressures are given for different collagen fiber orientations or stiffness. Furthermore, the stability of the solutions is discussed to explain the formation of aneurysm.

Keyword: artery, collagen fibers, aneurysm, incompressible anisotropic hyperelastic material, stress distribution, material instability

1 Introduction

Arterial aneurysms are focal dilatations of the arterial wall in or near bifurcations within the primary network of vessels that supply blood. In recent years, more and more people in the

world suffer aneurysms with asymptomatic lesions. Risk factors, such as hypertension, heavy alcohol consumption, cigarette smoking and long term use of analgesics, oral contraceptives or cocaine, may lead to the formation of aneurysms (Humphrey 2002, Humphrey 2003b). Beginning as a small dilatation of the arterial wall, aneurysms may expand much large and become complex in shape along with rapidly expanding lesions as shown in Fig. 1 (Watton et al 2004). Finally, aneurysms might in some cases rupture and this will give rise to devastating consequences. Rupture of aneurysm implies two outcomes such as significant bleeding and the formation of an intraluminal or intramural thrombus (He et al 1993, Lanne et al 1992, Papahariluon et al 2006). So aneurysms continue to be the cause of significant morbidity and mortality. Clearly, there is a need to combine geometrical, mechanical and histological methods to understand the mechanism of aneurysms comprehensively (Humphrey 2003b, Watton et al 2004, Wilmink et al 1995). And it is helpful for development of soft tissue biomechanics and tissue engineering (Neren and Selihhtar 2001).

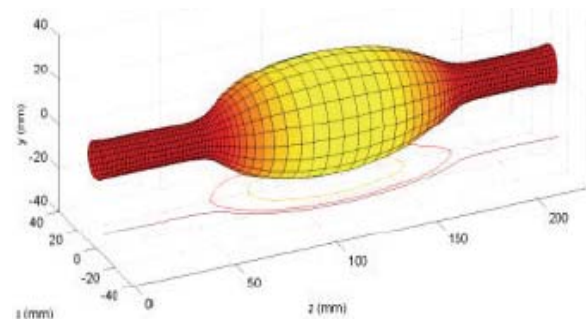


Figure 1: Schematic representation of an aneurysm (modified from Watton et al 2003)

* Department of Mechanics, Shanghai institute of applied Mathematics and Mechanics, Shanghai University, Shanghai 200444, China

From the point of histological view, soft biologi-

cal tissues such as arteries consist of various cell types and the extracellular matrix (Holzapfel et al 2004). The latter one is composed of proteins such as fibrous collagen and elastin. Structurally, for typical fiber architecture in an artery, the collagen fibers constitute symmetrically arranged helices (Holzapfel et al 1998, Holzapfel et al 2000, Driessen et al 2003). As shown in Fig. 2, the collagen fibers of the arterial wall are arranged in two helically distributed families with a small pitch and very little dispersion in their orientation (Humphrey 1995, Driessen et al 2004).

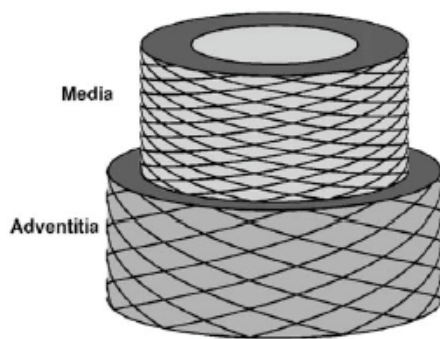


Figure 2: Schematic representation of typical fiber architecture in an artery (Holzapfel et al 2000, with a modification by Driessen et al 2004)

The constitutive response of soft tissue is an important prerequisite for analysis of the mechanical behavior of musculoskeletal system. But the behavior of soft tissue is complex, and it is often difficult to characterize (Olsen et al 1999, Holzapfel et al 2002). In addition to undergoing large strains, soft tissues exhibit time-dependent behavior and can actively contract, grow and remodel (Humphrey 2002). However, for many types of soft tissues, there is a characteristic, called pseudoelasticity (Fung 1990, Ogden 2002), that allows the use of nonlinear elasticity theory to study as a first approximation. And in practice, most researches, more commonly, simply assume that the material is elastic with constitutive relation based only on the loading curves. This approach has provided useful approximate results in a large number of problems although not strictly. The mechanical behavior of soft tissue under quasi-static loading is dominated by the perfor-

mance of its fibrous components, primarily collagen and elastin fibers. So, it is necessary to address how the collagen will remodel as the arterial wall dilates (Holzapfel et al 2003). Collagen fibers are often modeled as microscopic cylinders with a preferred direction and assumed to have mechanical characteristics independent of the configuration at which they are recruited (Humphrey 1999, Humphrey 2003a). Most of the researchers also assume that the predicted principal collagen fiber direction coincide with the principal strain direction within the valve tissue. However, the principal strain directions are in general oriented axially and circumferentially in blood vessels (Gasser et al 2006). As a result, continuum models that do not account for the dispersion between the directions of the principal strains and principal stresses are not able to capture accurately the stress-strain behavior of arteries. Ogden (Ogden 2003) gave the general stress-strain constitutive relation for arterial walls with collagen fibers distributed in two preferred directions. Holzapfel, Ogden and Gasser (Holzapfel et al 2000) proposed a hyperelastic model for arterial walls with collagen fibers distributed in two preferred directions. Guo et al (Guo et al 2006) developed a composites based hyperelastic constitutive model for arterial walls with collagen fibers distributed in two preferred directions which is used to model the annulus fibrosus. In the model proposed by Holzapfel et al (Holzapfel et al 2000), the preferred fiber directions and their changes depend on the magnitude of the principal stretches, which may explain the interrelation between the collagen architecture and the mechanical loading conditions.

The purpose of the present paper is to further investigate the formation, enlargement and rupture of aneurysm for arterial walls with collagen fibers distributed in two preferred directions using the nonlinear elastic theory. Based on the fiber-reinforced composite material model developed by Holzapfel et al (Holzapfel et al 2000) and view the artery as a two layer thick-walled tube, the stabilities of the artery is investigated in detail. At the normal condition, the artery wall undergoes a uniform inflation. But in some cases, when

the stiffness of the collagen fibers is damaged or the directions of the collagen fibers are changed, the artery wall may experience a strikingly non-uniform deformation. One portion of the artery becomes highly distended as a bubble while the rest remains lightly inflated. That is to say, an aneurysm is formed in the artery. Stretch-inflation pressure curves along with the critical pressures are given with different axial stretch and different collagen fiber stiffness. Furthermore, the distribution and the change of stresses are discussed. Finally, the rupture of aneurysm along with the deformation of aneurysm is discussed. The stability of the solutions is discussed, and the formation of the aneurysm is analyzed as a result of material instability.

2 Constituent relations

Typical architecture of an artery wall is shown in Fig. 2, the collagen fibers of the arterial wall are arranged in two helically distributed families with a small pitch and very little dispersion in their orientation. Based on the study of Driessen et al (Driessen et al 2004), the arterial wall is modeled as an incompressible fiber-reinforced composite material, in which the collagen fibers are viewed as a one-dimensional material, exerting only stress in the fiber direction, and the corresponding constitutive equation is derived from hyperelasticity. With the assumption of the incompressible matrix and fiber of the artery, the strain energy function of the artery can be expressed as

$$W = W_M + W_F \quad (1)$$

in which, W_M is the strain energy of the matrix and here is described by the incompressible Ogden hyperelastic material (Haugton et al 1978)

$$W_M = \sum_r \frac{\mu_r}{\alpha_i} (\lambda_r^{\alpha_r} + \lambda_\theta^{\alpha_r} + \lambda_z^{\alpha_r} - 3) \quad (2)$$

in which, $\alpha_1 = 1.3$, $\alpha_2 = 5.0$, $\alpha_3 = -2.0$, $\mu_1 = 1.491\mu$, $\mu_2 = 0.003\mu$, $\mu_3 = -0.023\mu$. μ is the shear modulus for the artery wall, λ_r , λ_θ , λ_z are the principal stretches. W_F is the strain energy of the collagen fiber and is described by the following express introduced by Driessen et al (Driessen

et al 2004)

$$W_F = \frac{k_1}{2k_2} e^{k_2(\lambda^2-1)^2} \quad (3)$$

in which, λ is the fiber stretch. Material constant k_1 is the stiffness of the collagen fiber and k_2 describes the degree of nonlinearity of the collagen fiber. The Cauchy stress is written as

$$\boldsymbol{\sigma} = -p\mathbf{I} + \boldsymbol{\tau}(\mathbf{B}) + \sum_{j=1}^2 \psi_f^j(\lambda_j^2) \mathbf{e}_f^j \mathbf{e}_f^j \quad (4)$$

where p is the hydrostatic pressure, \mathbf{I} is the unit tensor, $\boldsymbol{\tau}$ is the isotropic matrix stress, $\psi_f = 2k_1\lambda^2(\lambda^2-1)e^{k_2(\lambda^2-1)^2}$ is the fiber stress, $\mathbf{B} = \mathbf{F} \cdot \mathbf{F}^T$ is the left Cauchy-Green deformation tensor, \mathbf{F} is the deformation-gradient tensor corresponding to the deformation function, \mathbf{e}_f ($j = 1, 2$) is the fiber direction in the deformed configuration. It is assumed that $\boldsymbol{\tau}$ represent the contribution of all matrix components, except the collagen fibers, to the total constitutive behavior.

The fiber stretch is calculated from

$$\lambda = \sqrt{\mathbf{e}_{f0} \cdot \mathbf{C} \cdot \mathbf{e}_{f0}} \quad (5)$$

Here, \mathbf{e}_{f0} is the fiber direction in the undeformed configuration and $\mathbf{C} = \mathbf{F}^T \cdot \mathbf{F}$ is the right Cauchy-Green deformation tensor. The fiber direction in the deformed configuration is determined from that in the undeformed configuration

$$\lambda \mathbf{e}_f = \mathbf{F} \mathbf{e}_{f0} \quad (6)$$

3 Formulations

An artery subjected to combined internal inflation pressure and axial stretch may be considered as the inflation and extension of a two layer tube with inner radius a and outer radius b . The media and the adventitia of the artery are conglutinated at the interface with radius d ($a < d < b$) with the contribution of the intima is neglected. Assume that the undeformed and deformed configurations are described by the cylindrical coordinate systems (R, Θ, Z) and (r, θ, z) , respectively (as shown in Fig. 3). The deformation function of the tube is

$$r = r(R) > 0, \quad a \leq R \leq b, \quad \theta = \Theta, \quad z = \lambda_z Z$$

(7)

Where, $r(R)$ is a function to be determined, λ_z is the axial stretch ratio of the tube.

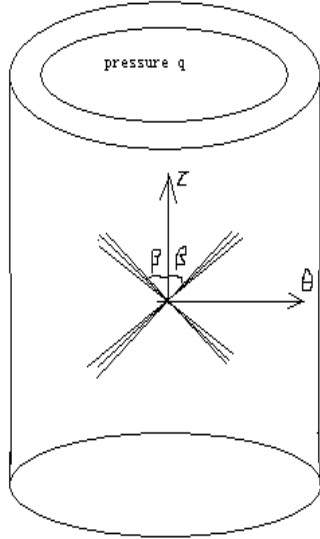


Figure 3: Schematic representation of the tube and fiber orientation

The corresponding deformation-gradient tensor \mathbf{F} is

$$\mathbf{F} = \text{diag}(\dot{r}(R), r(R)/R, \lambda_z) = \text{diag}(\lambda_r, \lambda_\theta, \lambda_z), \quad (8)$$

the corresponding principal stretches are

$$\lambda_r = \dot{r}(R) = dr/dR, \quad \lambda_\theta = r(R)/R, \quad \lambda_z = \lambda_z, \quad (9)$$

and the corresponding right or left Cauchy-Green deformation tensor is

$$\mathbf{C} = \mathbf{B} = \text{diag}(\dot{r}^2(R), r^2(R)/R^2, \lambda_z^2). \quad (10)$$

The equilibrium equation for the tube in the absence of body force is

$$\frac{d\sigma_{rr}^m}{dR} + \frac{\dot{r}(R)}{r(R)} [\sigma_{rr}^m - \sigma_{\theta\theta}^m] = 0, \quad (11a)$$

$$\frac{d\sigma_{rr}^a}{dR} + \frac{\dot{r}(R)}{r(R)} [\sigma_{rr}^a - \sigma_{\theta\theta}^a] = 0. \quad (11b)$$

where, $\sigma_{rr}^m, \sigma_{\theta\theta}^m, \sigma_{zz}^m$ represent Cauchy stress components of the media, and $\sigma_{rr}^a, \sigma_{\theta\theta}^a, \sigma_{zz}^a$ represent Cauchy stress components of the adventitia given by (4), respectively. Without special announcement in this paper, the superscript m denotes the media part when $a \leq R \leq d$ and the superscript a denotes the adventitia part when $d \leq R \leq b$. The boundary conditions are

$$\begin{aligned} \sigma_{rr}^m &= -q, & R &= a \\ \sigma_{rr}^a &= 0, & R &= b \end{aligned} \quad (12)$$

where, q is the inflation pressure applied on the inner surface.

From continuity of σ_{rr} at the interface of the media and the adventitia, it has

$$\sigma_{rr}^m = \sigma_{rr}^a, \quad R = d \quad (13)$$

The incompressibility condition of the material can be expressed as

$$r(R) = \left(\frac{1}{\lambda_z} (R^2 - a^2) + r^2(a) \right)^{\frac{1}{2}} \quad (14)$$

Letting

$$v = v(R) = \frac{r(R)}{R} = \left(\frac{1}{\lambda_z} \left(1 - \frac{a^2}{R^2} \right) + \frac{r^2(a)}{R^2} \right)^{\frac{1}{2}} \quad (15)$$

Then,

$$\lambda_\theta = v, \quad \lambda_r = \lambda_z^{-1} v^{-1} \quad (16)$$

Assume that the collagen fibers align with preferred directions \mathbf{e}_{f0}^i ($i = 1, 2$), directed among the principal stretch directions as shown in Fig.3. Then the directions for collagen fibers may be written as

$$\mathbf{e}_{f0}^1 = \begin{Bmatrix} 0 \\ \sin \beta \\ \cos \beta \end{Bmatrix}, \quad \mathbf{e}_{f0}^2 = \begin{Bmatrix} 0 \\ -\sin \beta \\ \cos \beta \end{Bmatrix} \quad (17)$$

Then, from (5), (10) and (17), it obtains

$$\lambda_1 = \lambda_2 = \lambda = \sqrt{\sin^2 \beta v^2 + \cos^2 \beta \lambda_z^2} \quad (18)$$

From (6), (17) and (18), we have

$$\mathbf{e}_f^1 = \frac{1}{\lambda} \begin{Bmatrix} 0 \\ \sin \beta v \\ \cos \beta \lambda_z \end{Bmatrix}, \quad \mathbf{e}_f^2 = \frac{1}{\lambda} \begin{Bmatrix} 0 \\ -\sin \beta v \\ \cos \beta \lambda_z \end{Bmatrix} \quad (19)$$

Here, the direction of collagen fibers β for the media and adventitia may take different values β_m and β_a in (17), (18) and (19). Then, from (4), non-zero Cauchy stresses for the media and adventitia are:

$$\begin{aligned} \sigma_{rr}^m(R) &= -p^m(R) \sum_r \mu_{\alpha_r}^m \lambda_z^{-\alpha_r} v^{-\alpha_r} \\ \sigma_{\theta\theta}^m(R) &= -p^m(R) \sum_r \mu_{\alpha_r}^m v^{\alpha_r} \\ &\quad + 4k_1^m (\lambda_m^2 - 1) e^{k_2^m (\lambda_m^2 - 1)^2} \sin^2 \beta_m v^2 \\ \sigma_{zz}^m(R) &= -p^m(R) \sum_r \mu_{\alpha_r}^m \lambda_z^{\alpha_r} \\ &\quad + 4k_1^m (\lambda_m^2 - 1) e^{k_2^m (\lambda_m^2 - 1)^2} \cos^2 \beta_m \lambda_z^2 \end{aligned} \quad (20a)$$

$$\begin{aligned} \sigma_{rr}^a(R) &= -p^a(R) \sum_r \mu_{\alpha_r}^a \lambda_z^{-\alpha_r} v^{-\alpha_r} \\ \sigma_{\theta\theta}^a(R) &= -p^a(R) \sum_r \mu_{\alpha_r}^a v^{\alpha_r} \\ &\quad + 4k_1^a (\lambda_a^2 - 1) e^{k_2^a (\lambda_a^2 - 1)^2} \sin^2 \beta_a v^2 \\ \sigma_{zz}^a(R) &= -p^a(R) \sum_r \mu_{\alpha_r}^a \lambda_z^{\alpha_r} \\ &\quad + 4k_1^a (\lambda_a^2 - 1) e^{k_2^a (\lambda_a^2 - 1)^2} \cos^2 \beta_a \lambda_z^2 \end{aligned} \quad (20b)$$

Substituting stresses (20a), (20b) into equation (11a), (11b) and integrating them over interval $[a, R]$, it has

$$-p^m(R) = \sum_r \mu_{\alpha_r}^m \lambda_z^{-\alpha_r} v^{-\alpha_r} + p^m(a) + J^m(R) = 0 \quad (21a)$$

$$-p^a(R) = \sum_r \mu_{\alpha_r}^a \lambda_z^{-\alpha_r} v^{-\alpha_r} + p^a(a) + J^a(R) = 0 \quad (21b)$$

where,

$$\begin{aligned} J^m(R) &= \frac{1}{\lambda_z v^2 R} \int_a^R \left[\sum_r \mu_{\alpha_r}^m (\lambda^{-\alpha_r} v^{-\alpha_r} - v^{\alpha_r}) \right. \\ &\quad \left. - 4k_1^m (\lambda_m^2 - 1) e^{k_2^m (\lambda_m^2 - 1)^2} \sin^2 \beta_m v^2 \right] dR \end{aligned}$$

$$\begin{aligned} J^a(R) &= \frac{1}{\lambda_z v^2 R} \int_a^R \left[\sum_r \mu_{\alpha_r}^a (\lambda^{-\alpha_r} v^{-\alpha_r} - v^{\alpha_r}) \right. \\ &\quad \left. - 4k_1^a (\lambda_a^2 - 1) e^{k_2^a (\lambda_a^2 - 1)^2} \sin^2 \beta_a v^2 \right] dR \\ &\quad + \frac{1}{\lambda_z v^2 R} \int_d^R \left[\sum_r \mu_{\alpha_r}^a (\lambda^{-\alpha_r} v^{-\alpha_r} - v^{\alpha_r}) \right. \\ &\quad \left. - 4k_1^a (\lambda_a^2 - 1) e^{k_2^a (\lambda_a^2 - 1)^2} \sin^2 \beta_a v^2 \right] dR \end{aligned}$$

Substituting (21a) and (21b) into stresses (20a) and (20b) and using the continuity condition of σ_{rr} at the interface of the media and the adventitia, we have

$$p^m(a) = p^a(a) = p(a) \quad (22)$$

Using the boundary conditions (12), we have

$$\begin{aligned} q &= \int_{v(a)}^{v(d)} \left[\sum_r \mu_{\alpha_r}^m (\lambda_z^{-\alpha_r - 1} v^{-1 - \alpha_r} - v^{\alpha_r - 1} \lambda_z^{-1}) \right. \\ &\quad \left. - 4k_1^m (\lambda_m^2 - 1) e^{k_2^m (\lambda_m^2 - 1)^2} \sin^2 \beta_m \lambda_z^{-1} v \right] \\ &\quad \left/ [\lambda_z^{-1} - v^2] \cdot dv \right. \\ &\quad + \int_{v(d)}^{v(b)} \left[\sum_r \mu_{\alpha_r}^a (\lambda_z^{-\alpha_r - 1} v^{-1 - \alpha_r} - v^{\alpha_r - 1} \lambda_z^{-1}) \right. \\ &\quad \left. - 4k_1^a (\lambda_a^2 - 1) e^{k_2^a (\lambda_a^2 - 1)^2} \sin^2 \beta_a \lambda_z^{-1} v \right] \\ &\quad \left/ [\lambda_z^{-1} - v^2] \cdot dv \right. \end{aligned} \quad (23)$$

In which, $v(b) = \left(\frac{1}{\lambda_z} \left(1 - \frac{a^2}{b^2} \right) + \frac{r^2(a)}{b^2} \right)^{\frac{1}{2}}$, $v(a) = \frac{r(a)}{a}$. It is an exact analytic relation between the stretch of the tube and the inflation pressure.

The corresponding non-zero principal stresses are

$$\begin{aligned}\sigma_{rr}^m &= -q \\ &- \int_{v(a)}^{v(R)} \left[\sum_r \mu_{\alpha_r}^m (\lambda_z^{-\alpha_r-1} v^{-1-\alpha_r} - v^{\alpha_r-1} \lambda_z^{-1}) \right. \\ &- 4k_1^m (\lambda_m^2 - 1) e^{k_2^m (\lambda_m^2 - 1)^2} \sin^2 \beta_m \lambda_z^{-1} v \left. \right] \\ &/ [\lambda_z^{-1} - v^2] \cdot dv \\ \sigma_{\theta\theta}^m &= \sum_r \mu_{\alpha_r}^m (v^{\alpha_r} - \lambda_z^{-\alpha_r} v^{-\alpha_r}) \\ &+ 4k_1^m (\lambda_m^2 - 1) e^{k_2^m (\lambda_m^2 - 1)^2} \sin^2 \beta_m v^2 + \sigma_{rr}^m \\ \sigma_{zz}^m &= \sum_r \mu_{\alpha_r}^m (\lambda_z^{\alpha_r} - \lambda_z^{-\alpha_r} v^{-\alpha_r}) \\ &+ 4k_1^m (\lambda_m^2 - 1) e^{k_2^m (\lambda_m^2 - 1)^2} \cos^2 \beta_m \lambda_z^2 + \sigma_{rr}^m\end{aligned}\quad (24a)$$

$$\begin{aligned}\sigma_{rr}^a &= -q \\ &- \int_{v(a)}^{v(d)} \left[\sum_r \mu_{\alpha_r}^a (\lambda_z^{-\alpha_r-1} v^{-1-\alpha_r} - v^{\alpha_r-1} \lambda_z^{-1}) \right. \\ &- 4k_1^a (\lambda_a^2 - 1) e^{k_2^a (\lambda_a^2 - 1)^2} \sin^2 \beta_a \lambda_z^{-1} v \left. \right] \\ &/ [\lambda_z^{-1} - v^2] \cdot dv \\ &- \int_{v(d)}^{v(R)} \left[\sum_r \mu_{\alpha_r}^a (\lambda_z^{-\alpha_r-1} v^{-1-\alpha_r} - v^{\alpha_r-1} \lambda_z^{-1}) \right. \\ &- 4k_1^a (\lambda_a^2 - 1) e^{k_2^a (\lambda_a^2 - 1)^2} \sin^2 \beta_a \lambda_z^{-1} v \left. \right] \\ &/ [\lambda_z^{-1} - v^2] \cdot dv \\ \sigma_{\theta\theta}^a &= \sum_r \mu_{\alpha_r}^a (v^{\alpha_r} - \lambda_z^{-\alpha_r} v^{-\alpha_r}) \\ &+ 4k_1^a (\lambda_a^2 - 1) e^{k_2^a (\lambda_a^2 - 1)^2} \sin^2 \beta_a v^2 + \sigma_{rr}^a \\ \sigma_{zz}^a &= \sum_r \mu_{\alpha_r}^a (\lambda_z^{\alpha_r} - \lambda_z^{-\alpha_r} v^{-\alpha_r}) \\ &+ 4k_1^a (\lambda_a^2 - 1) e^{k_2^a (\lambda_a^2 - 1)^2} \cos^2 \beta_a \lambda_z^2 + \sigma_{rr}^a\end{aligned}\quad (24b)$$

4 Results

Expression (23) gives the stretch-inflation pressure curves of the tube for given values of axial stretches and fiber directions as shown in Fig. 4~9. The geometrical and material parameters as well as the loading conditions used in calculations are taken from Holzapfel et al 2000 and Driessen et al 2003 for healthy youths arterial wall. The reference values of the initial fiber directions of the artery are taken from Holzapfel et al 2002. The reference values are summarized in Table 1. The internal pressure level is varied from 13.0 ~ 20.0kPa and the axial stretch is varied from 1.2 ~ 1.6.

As shown in Fig. 4, at the normal condition, the stretch-inflation pressure curve does not exhibit a maximum, and it means that no obvious instability can occur. That is to say, the artery wall takes up a uniform inflation deformation and there are no aneurysms in the artery at the normal condition. This is coincident with the clinical or experiment observations (Chyatte, Bruno, Desai, Tordor et al and Humphrey 2003). So we need to consider situations of imposed abnormal conditions, such as the change of the stiffness and directions of the fibers, the shear modulus of the matrix and the axial stretch. These changes can take place due to ages and vascular disease or disorders (Holzapfel and Ogden 2003 and Humphrey 2003a). The effects of age and disease on the artery are reflected by different values of material parameters for the strain energy function of the artery.

It is found that decrease of the shear modulus of the matrix does not also gives rise to instability (Fig. 4), and the main difference of the curves with respect to the normal condition is at its small strain deformation stage, i.e., the matrix bears the main part of the load at the small strain deformation stage, while the fibers bear the main part of the load at the large strain deformation stage.

The stretch-inflation pressure curve changes with the change of the directions of fibers when the fibers orientation towards the circumferential direction. The curve generally exhibits a maximum, and it means that an instability may occur

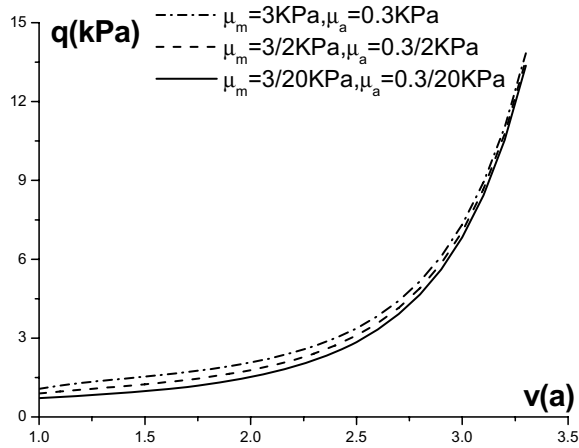


Figure 4: Stretch-inflation pressure curves for different shear modulus of the artery

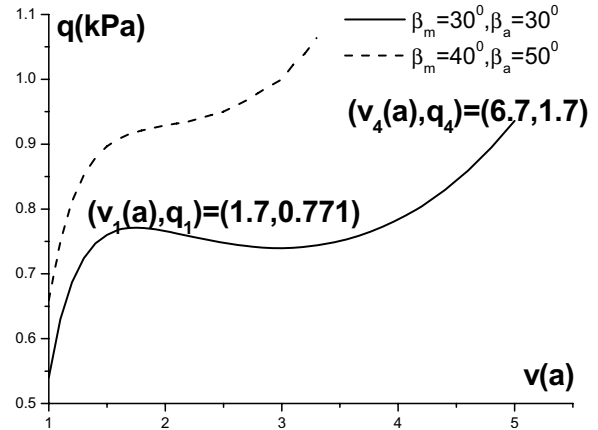


Figure 5: Stretch-inflation pressure curves for different directions of collagen fibers

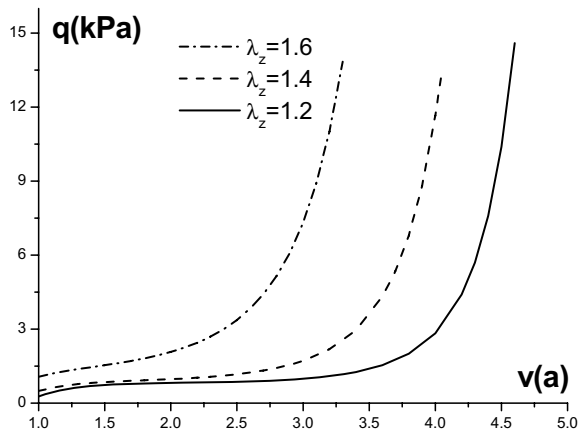


Figure 6: Stretch-inflation pressure curves for different axial stretch ratios

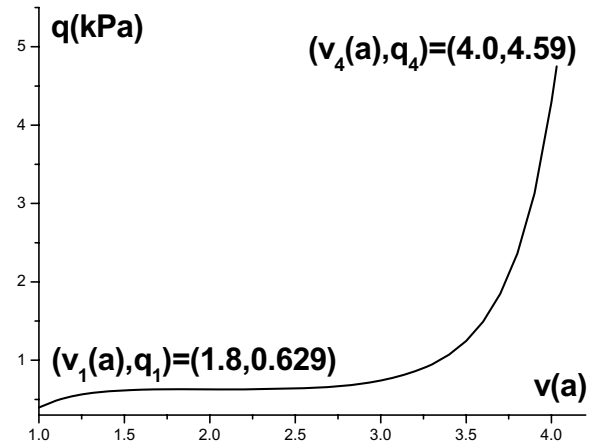


Figure 7: Stretch-inflation pressure curve ($k_{1m} = 1.18/30\text{kPa}$, $k_{1a} = 0.28/30\text{kPa}$)

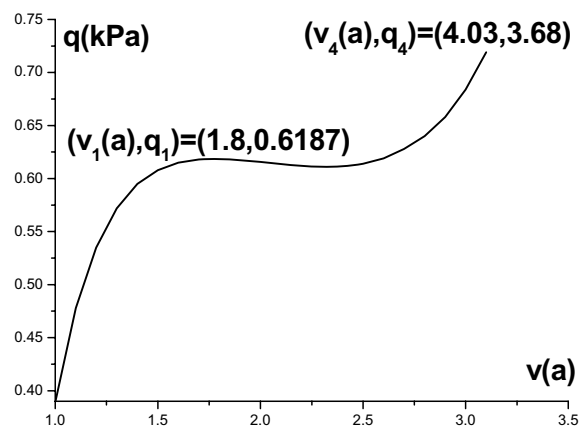


Figure 8: Stretch-inflation pressure curve ($k_{1m} = 1.18/40\text{kPa}$, $k_{1a} = 0.28/40\text{kPa}$)

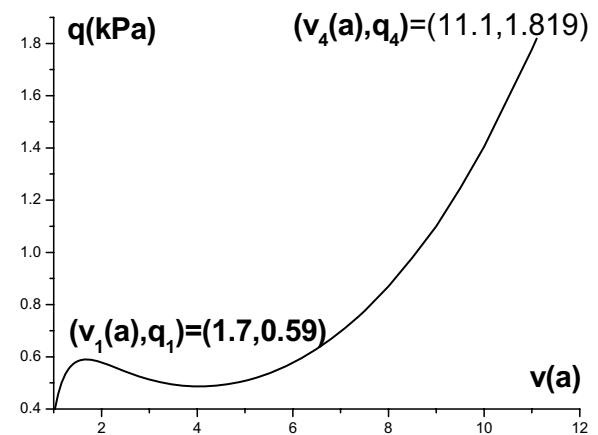


Figure 9: Stretch-inflation pressure curve ($k_{1m} = 0\text{kPa}$, $k_{1a} = 0\text{kPa}$)

Table 1: The reference values of the parameters used in the model

Parameter	Description	Value
a	Inner radius (undeformed configuration)	0.71mm
d	Interface for the media and adventitia	0.97mm
b	Outer radius	1.1mm
μ_m	Shear modulus for the media	3.0kPa
μ_a	Shear modulus for the adventitia	0.3kPa
k_{1m}	Fiber parameter for the media	1.18 kPa
k_{1a}	Fiber parameter for the adventitia	0.28 kPa
k_{2m}	Fiber parameter for the media	0.84
k_{2a}	Fiber parameter for the adventitia	0.71
q	Internal pressure	13.0 kPa
λ_z	Axial stretch	1.6~1.2
β_m	Initial fiber direction for the media	80°
β_a	Initial fiber direction for the adventitia	50°

as shown in Fig. 5. It is revealed that there exist a maximum inflation pressure q_1 ($v = v_1$) and a minimum pressure q_2 ($v = v_2$) on the stretch-inflation pressure curve. When the pressure is less than the maximum pressure, circumferential stretch of the tube increases slowly with the increasing of pressure. But when the pressure is larger than this maximum pressure, the stretch will increase rapidly. Finally, when the pressure reaches the minimum pressure, it increases with the increasing of pressure again.

Curves do not generally exhibit a maximum, and there is no obvious instability in the cases when the axial stretch is changed as shown in Fig. 6. For a certain direction of the fiber, the stiffness of the artery increases with the increasing of axial stretch. At the same pressure, the inflation deformation of the artery decreases with the increasing of the axial stretch. That is to say, the mechanical properties are mainly determined by the collagen fibers in the high pressure domain, which is accord with the main results of Driessen (Driessen et al 2003).

The curves generally exhibit a maximum, and there will be an obvious instability with highly reduced fiber stiffness as shown in Fig. 7~9. The maximum inflation pressure q_1 decreases with the decreasing of the stiffness of the fibers in this case.

Expressions of (24a) and (24b) yield the distri-

bution of stresses for the tube. Distribution of stresses for a certain state ($\lambda_z = 1.6$, $\beta_m = 80^\circ$, $\beta_a = 50^\circ$, $q = 0.74\text{kPa}$, $v(a) = 3.4$) is shown in Fig. 10. Fig. 11 and Fig. 12 show the increases of stresses with the increasing of stretch in the cases of $\lambda_z = 1.6$, $k_{1m} = k_{1a} = 0\text{kPa}$ and $\lambda_z = 1.6$, $k_{1m} = 1.18/30\text{kPa}$, $k_{1a} = 0.28/30\text{kPa}$, respectively. It is shown that the circumferential stress and the axial stress decrease with the increasing of radius, and they are discontinuous with a catastrophic jumping at the interface of the media and the adventitia. The radial stress increases with the increasing of radius, equaling to zero at the outer interface, and is continuous. At the same time, all the stress components increase with the increasing of stretch. The circumferential stress increases most rapidly in the case of $\lambda_z = 1.6$, $k_{1m} = k_{1a} = 0\text{kPa}$ and both the circumferential stress and the axial stress increase most rapidly in the case of $\lambda_z = 1.6$, $k_{1m} = 1.18/30\text{kPa}$, $k_{1a} = 0.28/30\text{kPa}$.

As shown in the stretch-inflation pressure curves of the tube in the Fig. 5, Fig. 7, Fig. 8 and Fig. 9, there exist one or more solutions corresponding to different inflations for a certain pressure, so that instability is encountered, and it is necessary to compare the total potential energy for the tube. The total potential energy of the inflated tube with internal pressure from the initial stress-free state

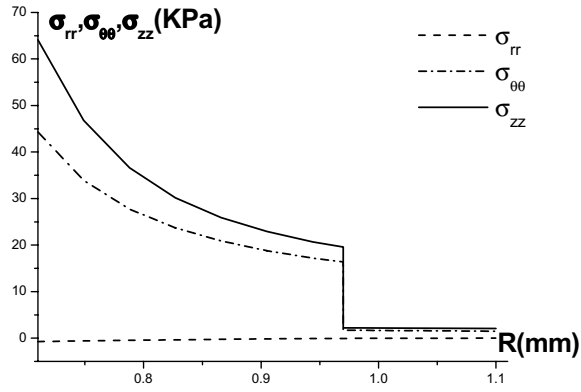


Figure 10: Stress distribution ($q = 0.74\text{kPa}$, $\lambda = 3.4$)

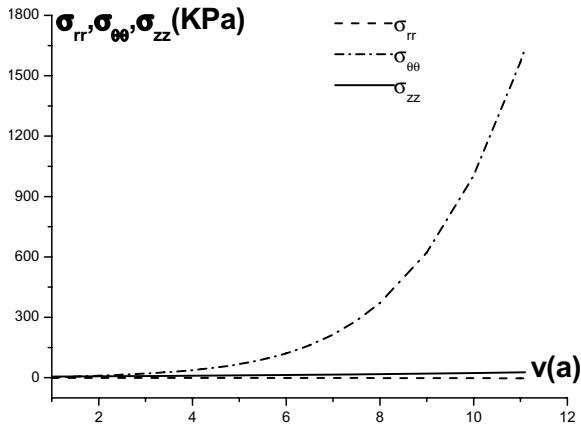


Figure 11: Increase of stresses ($\lambda_z = 1.6$, $k_{1m} = 0\text{kPa}$, $k_{1a} = 0\text{kPa}$)

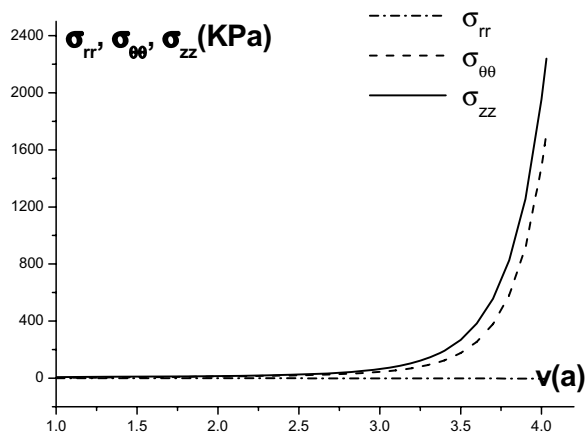


Figure 12: Increase of stresses ($\lambda_z = 1.6$, $k_{1m} = 1.28/30\text{kPa}$, $k_{1a} = 0.28/30\text{kPa}$)

is

$$\begin{aligned}
 E &= \int_V W dV - \int_A q(r(a) - a) dA \\
 &= 2\pi L \int_a^b RW dR - \pi L \frac{a+r(a)}{2} q(r(a) - a) \\
 &= 2\pi La^2 (v^2(a) - \lambda_z^{-1}) \\
 &\quad \cdot \left(\int_{v(d)}^{v(a)} \frac{W_m v}{(\lambda_z^{-1} - v^2)^2} dv + \int_{v(b)}^{v(d)} \frac{W_a v}{(\lambda_z^{-1} - v^2)^2} dv \right) \\
 &\quad - \pi La^2 q (v^2(a) - 1)
 \end{aligned} \tag{25}$$

Numerical result of (25) for the inflation tube in the case of $\lambda_z = 1.0$, $k_1 = 0$ is shown in Fig. 14. The corresponding stretch-inflation pressure curve is shown in Fig. 15. It is shown that the total potential energy of the inflated tube decreases with the increasing of stretch when $1 \leq v(a) \leq v_1(a)$ or $v_2(a) \leq v(a)$. But it increases with the increasing of stretch when $v_1(a) \leq v(a) \leq v_2(a)$. The total potential energy at stretch $v_3(a) = 5.2$ is less than that at stretch $v_1(a) = 2.2$ under the same inflation pressure $q = 0.79\text{kPa}$. That is to say, the tube attained a stable deformation state when the pressure is less than the maximum pressure and takes up a uniform deformation. But when the pressure is larger than the maximum pressure, the deformation state is unstable. After a small inflation, the tube is subject to a complex deformation. One part of the tube becomes highly distended as a bubble while the rest remains lightly inflated (Gent 2002). It means that an aneurysm is formed in the artery as shown in Fig. 1. When the stretch reaches the value of $v_3(a) = 5.2$, the tube will attain a second stable deformation. The stretch will increase with the increasing inflation pressure again. That is to say the aneurysm will expand rapidly after this formation and will become complex in shape and constitution at first. Then it will expand to a certain extent until the finally rupture. This procedure is well agreement with the observation for intracranial saccular aneurysms described by Humphrey (Humphrey 2003b).

It is widely thought that if the stress induced

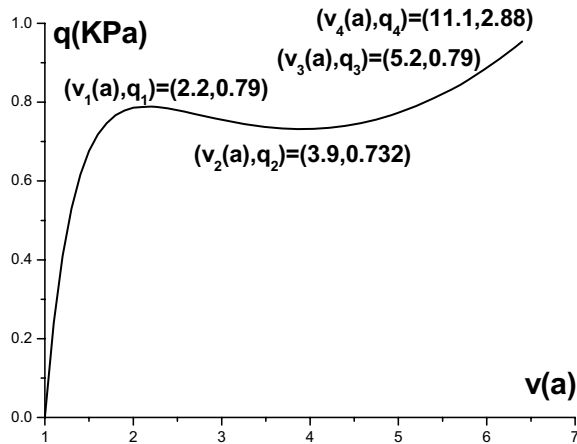


Figure 13: Stretch-inflation pressure curve ($\lambda_z = 1.0, k_{1m} = 0, k_{1a} = 0$)

by pressure is less than the strength of the artery wall, the aneurysm will keep its inflation state. But if this stress is larger than the strength of the artery wall, the rupture will occur (Humphrey 2003b). Based on the observation of Humphrey (Humphrey 2003b), two human secular aneurysms exhibited critical breaking stresses on the order of $\sigma_c = 1 \sim 2$ MPa, $\sigma_c = 1.6$ MPa is taken out to model the rupture of the aneurysm. The critical breaking point $(v_4(a), q_4)$ is shown on the stretch-inflation pressure curve for all the cases with the formation of aneurysm. It is shown that the normal blood pressure (13.0 \sim 20.0kPa) is large enough for the rupture of the aneurysm. That is to say the aneurysm will rupture after it is formed. But we may see that the demand rupture pressure increases with the increasing of the stiffness of the fibers. So there has the probability that the demand rupture pressure is larger than the normal blood pressure. Thus the aneurysm will keep its inflation state without the risk of rupture.

5 Discussions

From the above analyses, we can conclude that the formation and enlargement, even the rupture of the aneurysm in arteries with collagen fibers distributed in two preferred directions may be described by the model presented in the paper. An aneurysm may be formed in arteries with collagen fibers when the stiffness of the fibers is decreased

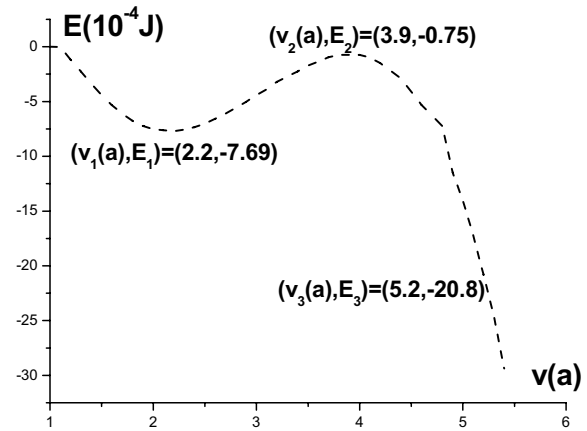


Figure 14: Energy curve ($\lambda_z = 1.0, k_{1m} = 0, k_{1a} = 0$)

to a certain value or the direction of the fibers is changed to a certain degree towards the circumferential direction due to ages or vascular diseases for certain people. The aneurysm may undergo an instable expand deformation, expand to much large extent and become complex in shape. Then the aneurysm may get a stable deformation for further enlargement when the stretch is larger than the certain value corresponding to the maximum pressure. Finally, the aneurysm may catastrophically rupture when the demand failure pressure is less than the normal blood pressure.

The effect of collagen fibers distributed in the artery wall is remarkable. Both of the stiffness and the distribution direction of the collagen fibers affect on the formation, enlargement and rupture of the aneurysm. When the stiffness of the collagen fibers is reduced by some risk factors such as hypertension, heavy alcohol consumption, cigarette smoking, long term use of analgesics, oral contraceptives or cocaine, the stiffness of the artery decreased. So it is easier for an aneurysm to be formed and it will expand to a larger extent under the same condition.

When the collagen fibers orient towards the circumferential direction, the stiffness in the circumferential direction will be increased. So it is easier for an aneurysm to be formed at a small value of the fiber direction. When the axial stretch is increased, the stiffness of the whole aneurysm in-

creases with it (Peng 1999). Although the stiffness of the circumferential direction contributed by the fibers decreased because the fiber direction decreased, it is less than that increased. So the stiffness of the aneurysm increases with the increasing of axial stretch, and it is easier for an aneurysm to be formed at a small value of axial stretch.

These results have an obvious clinical application in those patients with aneurysms. The formation, enlargement and the rupture of the aneurysm is determined by different ages and health conditions of the people. The effects of age and disease on the artery are reflected by different values of material parameters for the strain energy function. But the relation between them requires increased physiological knowledge, more material constants and physiological data are demanded.

Acknowledgement: This work was supported by the National Nature Science Foundation of China (10402018), the youth foundation of the Education Commission of Shanghai (04AC90) and Shanghai Key Project Program (Y0103).

References

1. **Chyatte, D.; Bruno, G.; Desai, S.; Tordor, R.** (1999): Inflation and intracranial aneurysms. *Neurosurgery*, 45, 1137-1147.
2. **Driessen, N. J. B.; Peters, G. W. M.; Huyghe, J. M.** (2003): Remodeling of continuously distributed collagen fibers in soft connective tissues. *J. Biomech.*, 36(8), 1111-1158.
3. **Driessen, N. J. B., Wilson, W., Bouten, C. V. C.** (2004): A computational model for collagen fiber remodeling in the arterial wall. *J of Theoretical Biology*, 226, 53-64.
4. **Fung, Y. C.** (1990): *Biomechanics: Motion, Flow, Stress and Growth*. Springer-Verlag, New York.
5. **Gasser, T. C.; Ogden, R. W.; Holzapfel, G. A.** (2006): Hyperelastic modeling of arterial layers with distributed collagen fiber orientations. *J. R. Soc. Interface*, 3, 15-35.
6. **Gent, A. N.** (2005): Elastic instability in rubber. *Int. J. of Nonlinear Mechanics*, 40, 165-175.
7. **Guo, Z. Y.; Peng, X. Q.; Morun, B.** (2006): A composites-based hyperelastic constitutive model for soft tissue with application to the human annulus fibrosus. *J. of the Mechanics and Physics of Solids*, 54, 1952-1971.
8. **Haughton, D. M.; Ogden, R. W.** (1978): On the incremental equations in nonlinear elasticity-II: Bifurcation of pressurized spherical shells. *J. Mech. Phys. Solids*, 26, 111-138.
9. **He, C. M.; Roach, M.** (1993): The composition and mechanical properties of abdominal aortic aneurysms. *J Vasc. Surg.*, 20, 6-13.
10. **Holzappel, G. A.; Weizaker, H. W.** (1998): Biomechanical behavior of the arterial wall and its numerical characterization. *Comput. Bio. Med.*, 28, 377-393.
11. **Holzappel, G. A.; Gasser, T. C.; Ogden, R. W.** (2000): A new constitutive framework for arterial wall mechanics and a comparative study of material models. *J. of Elasticity*, 61, 1-48
12. **Holzappel, G. A.; Gasser, T. C.; Stadler, M.** (2002): Structural model for the viscoelastic behavior of arterial walls, continuum formulations and finite element analysis. *Eur. J. Mech. A/Solids*, 21(3), 441-463.
13. **Holzappel, G. A.; Ogden, R. W.** (2003): *Biomechanics of soft tissue in cardiovascular systems*. Wien Springer. *CISM courses and lectures*, 441.
14. **Holzappel, G. A.; Sommer, G.; Regitnig, P.** (2004): Anisotropic mechanical properties of tissue components in human atherosclerotic plaques. *J. Biomech. Eng.*, 126, 657-665.
15. **Humphrey, J. D.** (1999): Remodeling of a collagenous tissue at fixed lengths. *J. Biomech. Eng.*, 121(6), 591-597.

16. **Humphrey, J. D.; Canham, P. B.** (2000): Structure, mechanical properties and mechanics of intracranial saccular aneurysms. *J. of Elasticity*, 61, 49-81.
17. **Humphrey, J. D.** (2002): Cardiovascular solid Mechanics. Cells, Tissures and Organs. Springer-Verlag NewYork, New York.
18. **Humphrey, J. D.** (2003a): Intracranial saccular aneurysms. In: Holzapfel G.A., Ogden R.W. (ed.), Biomechanics of soft tissue in cardiovascular systems. Springer Wien-NewYork, New York, 185-220.
19. **Humphrey, J. D.** (2003b) Continuum biomechanics of soft biological tissues. *Proc. R. Soc. A.*, 459, 1-44.
20. **Lanne, T.; Sonesion, B.; Bergquist, D.** (1992): Diameter and compliance in the male human abdominal aorta: influence of age and aortic aneurysm. *Eur. J Vasc. Surg.*, 6, 178-189.
21. **Neren, R. M.; Selihtar, D.** (2001): Vascular tissue engineering. *Annu. Rev. Biomech. Eng.*, 3, 225-243.
22. **Ogden, R. W.** (2002): Pseudo-elasticity and stress softening. In: Fu Y. B., Ogden R. W.(ed.), Nonlinear Elasticity. Cambridge University Press. Cambridge, 491-522.
23. **Ogden, R. W.** (2003): Nonlinear elasticity, anisotropy, material stability and residual stresses in soft tissue. In: Holzapfel G.A., Ogden R.W.(ed.), Biomechanics of soft tissue in cardiovascular systems. Springer WienNewYork. New York, 65-108.
24. **Olsen, L.; Maini, P. K.; Sherratt, J. A.** (1999): Mathematical modeling of anisotropy fibrous connective tissue. *Math. Biosci.*, 15892, 145-170.
25. **Papahariluon, Y.** (2006): A decoupled fluid structure approach for estimating wall stress in abdominal aortic aneurysms. *J. Biomech.*, 39, 1111-1158.
26. **Peng, Y. H.; Li, X. Y.; Wu, S. G.** (1999): A data-processing technique for the 3D static nonlinear mechanical properties of arterial wall. *J. of Experiment Mechanics* (in Chinese). 14, 425-431.
27. **Schulze-Bauer, C. A. J.; Hozapfel, G. A.** (2003): Determination of constitutive equation for human arteries from clinical data. *J. of Biomechanics*, 36, 165-169.
28. **Watton, P. N.; Hill, N. A.; Heil, M.** (2004): A mathematical model for the growth of abdominal aortic aneurysm. *Biomechan Model Mechanobiol*, 3, 98-113.
29. **Wilmink, W. B. M.; Quick, C. R. G.; Hubbard, C. S.; Dag, N. E.** (1999): The influence of screening on the incidence of ruptured abdominal aortic aneurysms. *J Vasc. Surg.*, 30, 203-208.